Crystal rotation behavior with fatigue crack propagation in copper films

Kenichi SHIMIZU* and Tashiyuki TORII
Division of Industrial Innovation Sciences
The Graduate School of Natural Science and Technology,
Okayama University
3-1-1 Tsushima-naka, Okayama, Japan

Koki ISHIDA
Uchiyama Manufacturing Corp.
1106-11 Ohkanda, Akaiwa, Japan

Using a fatigue testing method by which fatigue cracks can be initiated and propagated in a film adhered to cover an elliptical through-hole in a base plate subjected to push-pull cyclic loads, annealed copper films with the thickness of 100μm and those reduced the thickness from the 100μm to 50μm by an electro-polishing were fatigued under a constant stress amplitude with a stress ratio of zero. The crystal rotation behavior with the fatigue crack propagation was investigated by measuring the crystal orientation around the fatigue crack initiated from the notch root before and after fatigue testing, using EBSD (Electron Back-scatter Diffraction) method. Then, the change of crystal orientation with fatigue testing was evaluated quantitatively from the misorientation between the crystal orientation matrix on the same point obtained before and after fatigue testing. As a result, the angle of the crystal rotation obtained from the region showing the high fatigue crack propagation rate was larger than that obtained from the region showing the low fatigue crack propagation rate for the film with the thickness of 100μm, while the fatigue crack propagated faster in the film with the thickness of 50μm than that with the thickness of 100μm regardless of the small crystal rotation angles with the fatigue testing for the film with the thickness of 50μm.

1. INTRODUCTION

In recent years, film materials are often used in electronic devices, such as the films deposited on rigid substrates[1] and on IC packages modeling a multi-layer construction [2,3]. For reliability of these parts, it is necessary to estimate the fatigue properties of the film materials, of which mechanical properties will be different from those of bulk materials used as relatively large-sized components of machines. However, since fatigue testing presents a serious difficulty with regard to gripping small specimens, the fatigue properties of the film specimen have been hardly discussed as compared with those of the bulk specimen. Therefore, the fatigue properties of bulk specimens are often used to design electronic parts in spite of the necessity for discussing about a difference in the fatigue fracture properties between the film and the bulk specimen.
In this study, a film fatigue testing method was proposed by which fatigue crack initiation and propagation occurred on a film bonded to a circular through-hole in a base plate subjected to push-pull cyclic loads[4,5]. If a film adhered to a through-hole in a base plate subjected to loading is regarded as the ellipsoidal inclusion in Eshelby's model[6], the strain and the stress will be uniform in the film. In this way, it is possible to conduct film fatigue testing by stress cycling on the base plate. Using this fatigue testing method of film, fatigue properties of the film with the thickness of 100μm and 50μm were examined for copper films annealed at 873 K. The crystal rotation behavior with the fatigue crack propagation was investigated by measuring the crystal orientation around the fatigue crack initiated from the notch root before and after fatigue testing, using EBSD (Electron Back-scatter Diffraction) method[7]. Then, the change of crystal orientation with fatigue testing was evaluated quantitatively from the misorientation between the crystal orientation matrix on the same point obtained before and after fatigue testing[8,9]. Finally, the effects of film thickness on fatigue fracture properties in the copper film was discussed from the analysis of the change of crystal orientation around the cracks with fatigue testing.

*E-mail: kshimizu@mech.okayama-u.ac.jp

2. EXPERIMENTAL PROCEDURE

2.1. Specimens

The cold rolled pure copper films with a thickness of t_f=100μm were annealed at 873 K for one hour in a vacuum furnace. The copper films of t_f=50μm thickness were made from those of 100μm thickness by electro-polishing and were annealed at 873 K for one hour. Figure 1 shows the optical micrographs observed from the cross section of copper films with the thickness of 100μm and 50μm. The number of grains per thickness are 3~4 for the film of t_f=100μm thickness and are 1~2 for the film of t_f=50μm thickness. The base specimens of medium carbon steels (S45C) were machined to the dimension with a circular through-hole shown in Fig. 2, then polished with emery paper and finally annealed at 1123 K for one hour in a vacuum furnace. A base plate with smooth surfaces for both sides was defined as the base plate "A", and that with a dent on one side was defined as the base plate "B". The thickness of both base plates was t_b=1.0mm. The chemical compositions of the film and the base plate are shown in Table 1. The film specimen was cut into a 30×30 mm^2 rectangle and a through-hole of 0.5 mm diameter was made at the film center by using a drilling machine. The film was bonded to the base plate "B" so that the rolling direction were parallel to the loading direction of the base plate as illustrated in Fig. 2. Finally, the base plate "A" was bonded to the film adhered to the base plate "B".

2.2 Film Fatigue Testing

The film was fatigued in accordance with the displacement along the hole circumference in the base plates subjected to push-pull sinusoidal cyclic loads with a constant stress amplitude, $(\sigma_a)_b$=35MPa, at a speed of 20 Hz and a stress ratio of $R = 0$, using a servo-hydraulic fatigue testing machine. In this fatigue testing, the cyclic strains and stresses are uniform in the film adhered to a through-hole in a base plate subjected to cyclic loading, as described in the ellipsoidal inclusion in Eshelby's model[6]. The stress distribution calculated using a three-dimensional elastic FEM analysis was almost uniform on the film, the value of which was almost 1.6 times of applied stress $(\sigma_a)_b$. The fatigue crack behavior on the film was observed using an optical microscope attached to the testing machine.

2.3 Crystal Orientation Analysis

The crystal orientation of copper films was analyzed using an EBSD system (Link OPAL, Oxford Instruments)[7]. The analyzed area was 128x168μm with the measured points of 100 x 128 =12800.

2.4 Calculation of Crystal Rotation Angle

Figure 3 illustrates the relationship between the crystal axes and the specimen axes. The cosines of α_1, β_1 and γ_1 are the angles between [100] and rolling direction, [100] and transverse direction and [100] and normal direction respec-

Table 1 Chemical compositions.

(mass %)

	Al	Ni	Sn	Pb	Fe	Zn	Mn
Pure copper (Film of 100μm thickness)	$5\times10^{-5}>$	$5\times10^{-5}>$	$5\times10^{-5}>$	$5\times10^{-5}>$	$5\times10^{-5}>$	$5\times10^{-5}>$	4×10^{-5}

	C	Si	Mn	P	S
Medium carbon steel (S45C) (Base plate)	0.45	0.18	0.78	0.012	0.006

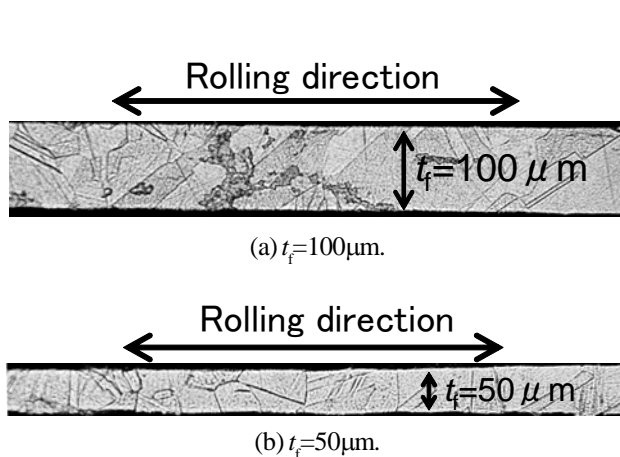
(a) t_f=100μm.

(b) t_f=50μm.

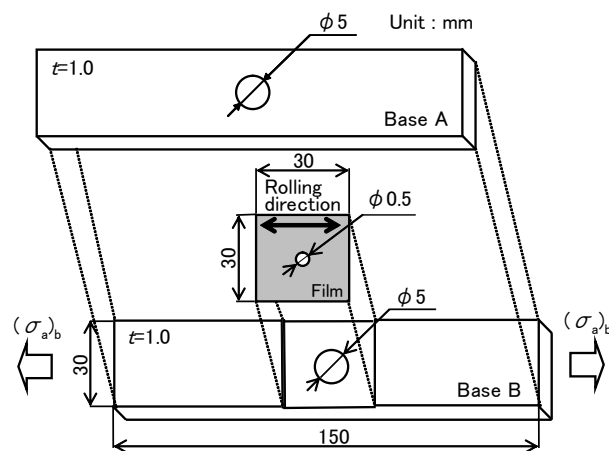Fig. 1 Microstructures on the cross section of the copper film.

Fig. 2 Dimension of the film fatigue specimen.

tively. They form the first row of the orientation matrix, A, as shown in eq. (1). The other two rows are formed in a similar manner from the cosines of angles between [010] and rolling direction, [010] and transverse direction and [010] and normal direction; then [001] and rolling direction, [001] and transverse direction and [001] and normal direction. These angles are α_2, β_2, γ_2 and α_3, β_3, γ_3 respectively. For clarity only α_1, β_1, γ_1 are shown on Fig. 3.

$$A = \begin{pmatrix} \cos\alpha_1 & \cos\beta_1 & \cos\gamma_1 \\ \cos\alpha_2 & \cos\beta_2 & \cos\gamma_2 \\ \cos\alpha_3 & \cos\beta_3 & \cos\gamma_3 \end{pmatrix} \qquad (1)$$

When an orientation matrix obtained from a point before fatigue testing and that obtained from the same point after fatigue testing are defined as A_2 and A_1 respectively, the crystal rotation angle, θ, can be calculated as follows;

$$M_{21} = A_2^{-1} A_1 \qquad (2)$$

$$\cos\theta = \frac{\mathrm{Tr}M_{21} - 1}{2} \qquad (3)$$

where M_{21} is the matrix which represents the rotation of A_1 onto A_2, $\mathrm{Tr}M_{21}$ is the summation of the diagonal elements. The same point on COM (Crystal Orientation Map) obtained before fatigue testing, P_2, with that obtained after fatigue testing, P_1, is determined as shown in Fig. 4. A mask containing the point P_2 at the center is extracted from the COM obtained after fatigue testing and the summations of the misorientation angles calculated from each point with scanning the mask on the COM obtained before fatigue testing. The same point, P_1, is found at the minimum summation value of the misorientation angles.
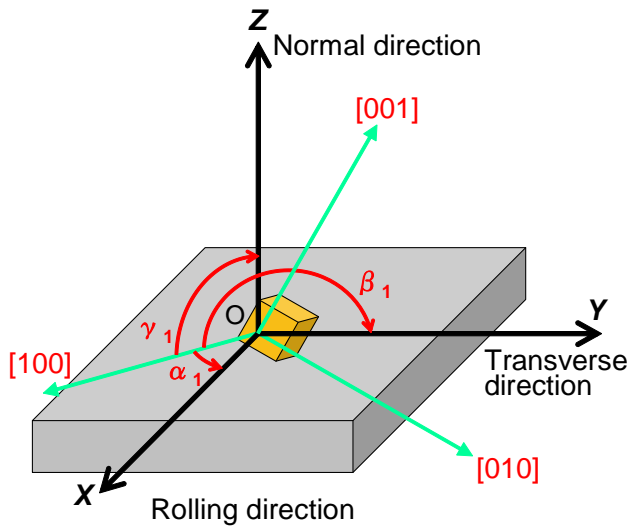
3. EXPERIMENTAL RESULTS AND DISCUSSIONS

3.1 Fatigue Crack Propagation

Figure 5 shows the crack propagation curves of the copper film. The crack propagates faster in the film of 50μm thickness than in that of 100μm thickness. It is shown that the periods of the crack arrest in the film of 100μm thickness is longer than in the film of 50μm thickness.

Figures 6 shows the surface crack observed through the use of a SEM (Scanning Electron Microscope) in the film of 100μm and 50μm thickness. Many slip lines are observed around the crack at the half-length of a>0.6 mm for both films of 100μm and 50μm thickness. While almost slip lines are localized near the fatigue crack in the film of 100μm thickness, large slip lines are scattered far from the fatigue crack in the film of 50μm thickness.

3.2 Crack Rotation with Fatigue Testing

Figure 7 shows the color key used to produce COM. The crystal orientation near the notch root expressed by a square in Fig. 6 was analyzed using EBSD technique. Fig-
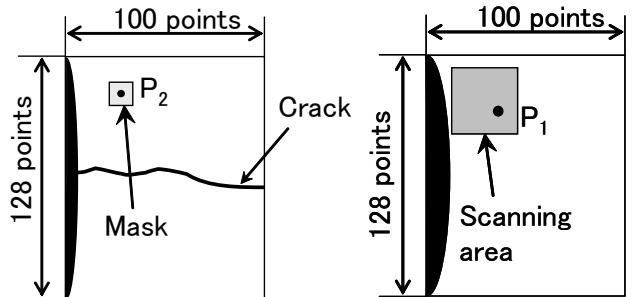
(a) Mask extracted from the region obtained after fatigue testing.

(b) Scannning area on the region obtained before fatigue testing.
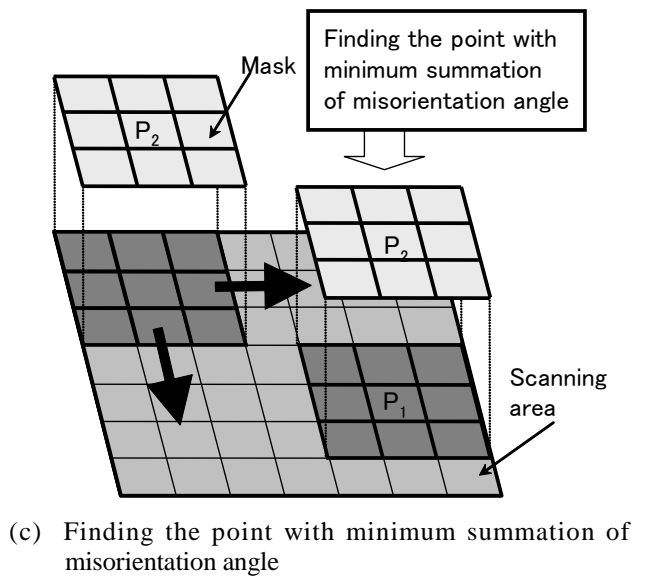
(c) Finding the point with minimum summation of misorientation angle

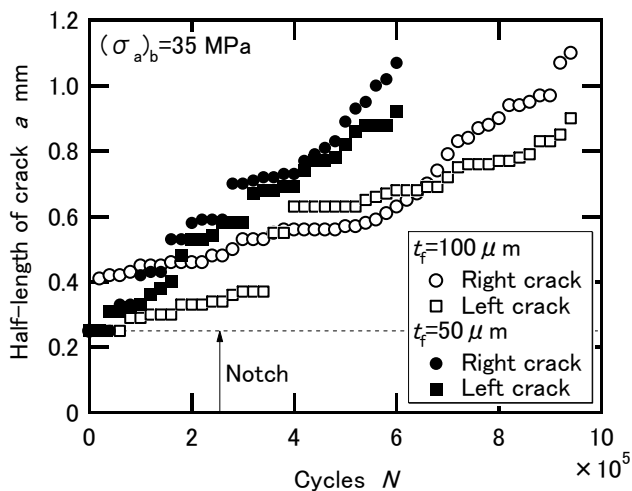Fig. 4 Explanation of the method to determine the same point before and after fatigue testing.

Fig. 3 Definition of specimen axes and crystal axes.

Fig. 5 Fatigue crack propagation curves.

ure 8 shows the mapping of crystal orientation to the normal direction by using colors indicated in the color key. As the point expressed by the same color has the same crystal orientation, it is likely to indicate a grain. From these figures, it is shown that the grain size ranges from 40mm to 100μm and some large grains of 200μm or larger can be seen in the film of 100μm and 50μm thickness. Straight boundaries are annealing twin boundaries with the misorientation angle between the neighboring grains of 60 degree. The fatigue cracks are expressed by white lines. It can be seen that the crack often propagated along the annealing twin boundary for both the film of 100mm and 50μm thickness. While the main crack propagates continuously in the film of 100μm thickness with short branched crack, the crack often propagates with branching and the coalescence around the grain boundary in the film of 50μm thickness.

Crack propagation direction
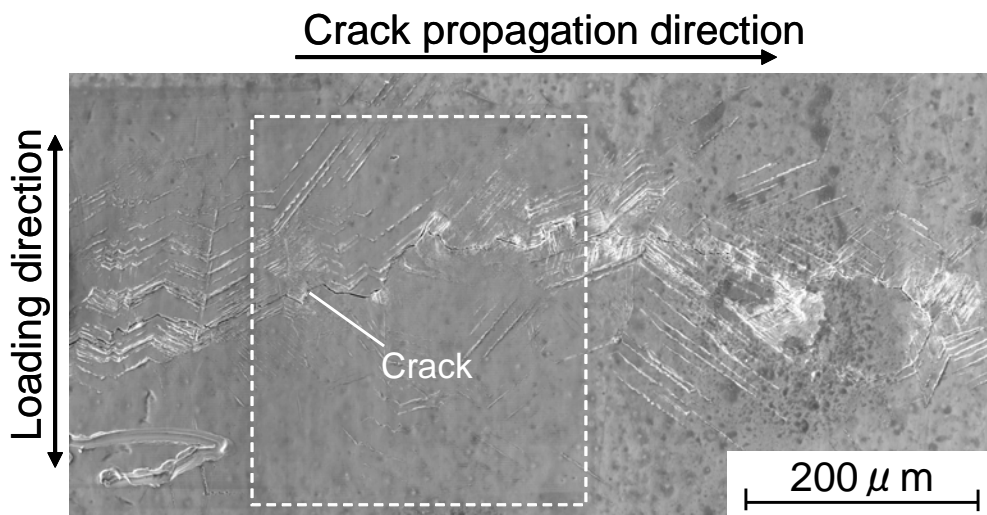
(a) t_f=100μm, right crack, a=1.10 mm, N=9.6$\times$10^5 cycles.

Crack propagation direction
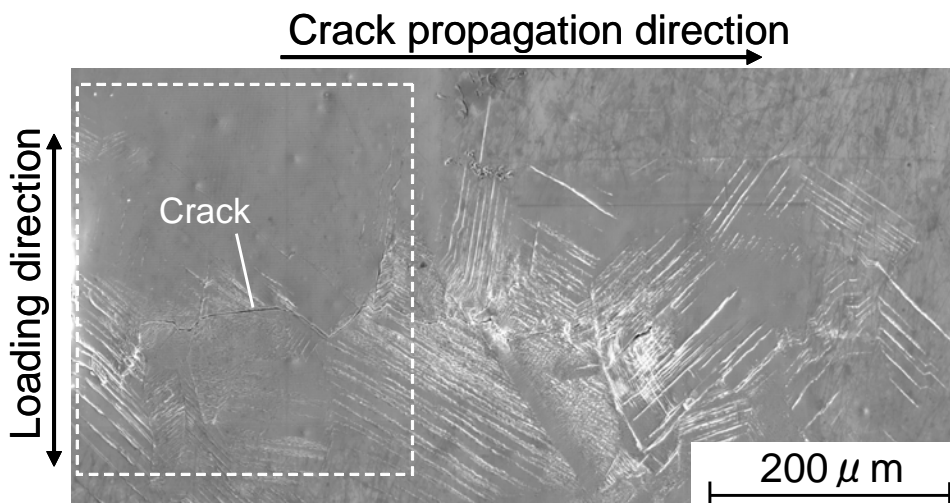
(b) t_f=50μm, left crack, a=0.92 mm, N=6.0$\times$10^5 cycles.

Fig. 6 SEM micrograph of fatigue crack in the film.

Figure 9 shows the distribution of the crystal rotation angle, θ, with fatigue testing. The area illustrated by black shows the region in which the crystal rotation angle is not able to be calculated for the severe damage on the film surface. The change of crystal orientation is remarkable near the fatigue crack in the film with the thickness of 100μm. On the other hand, the crystal rotation angle is relatively small even near the fatigue crack in the film of 50μm thickness and the crystal rotation angle is difference between the upper side and the lower side of the fatigue crack.
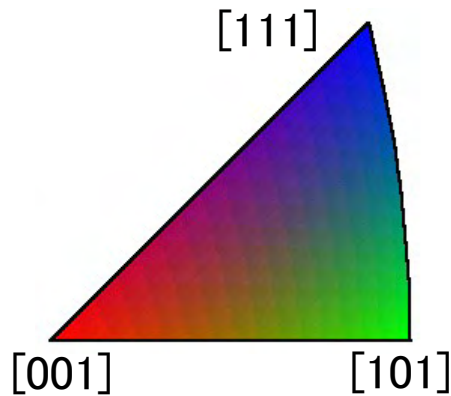
3.3 Roughness around the Fatigue Crack
Figure 10 shows the roughness around the fatigue crack measured by the confocal lazer scanning microscopy (Lasertec Corp., 1LM21). The measured area is almost the same with the crystal orientation mapping area as illustrated in Fig. 8. The film surface is piled up around the fatigue crack in the film with the thickness of 100μm. On the other hand, the difference in level is found across the fatigue crack in the film with the thickness of 50μm. Namely, it is considered that the deformation behavior with fatigue crack propagation is different between the film with the thickness of 100μm and that with the thickness of 50μm. From Fig. 1 of the microstructure observed from the cross section of the copper film with the thickness of 100μm and 50μm thickness, the restriction condition for the deformation toward the film thickness direction is seemed to be looser in the film of 50μm thickness with 1~2 grains existing on the cross section than in the film of 100μm thickness with 3~4 grains. The slip deformation is difficult to occur owing to the restriction condition in the film with the thickness of 100μm and the crystal rotation results on behalf of the slip deformation. On the other hand, the difference in level across the fatigue crack is considered to be caused by the slip deformation in the film with the thickness of 50μm. Because of the weak restricton condition for the deformation, the slip deformation occures easily without crystal rotation in the film of 50μm thickness. In

Fig. 7 Color key.
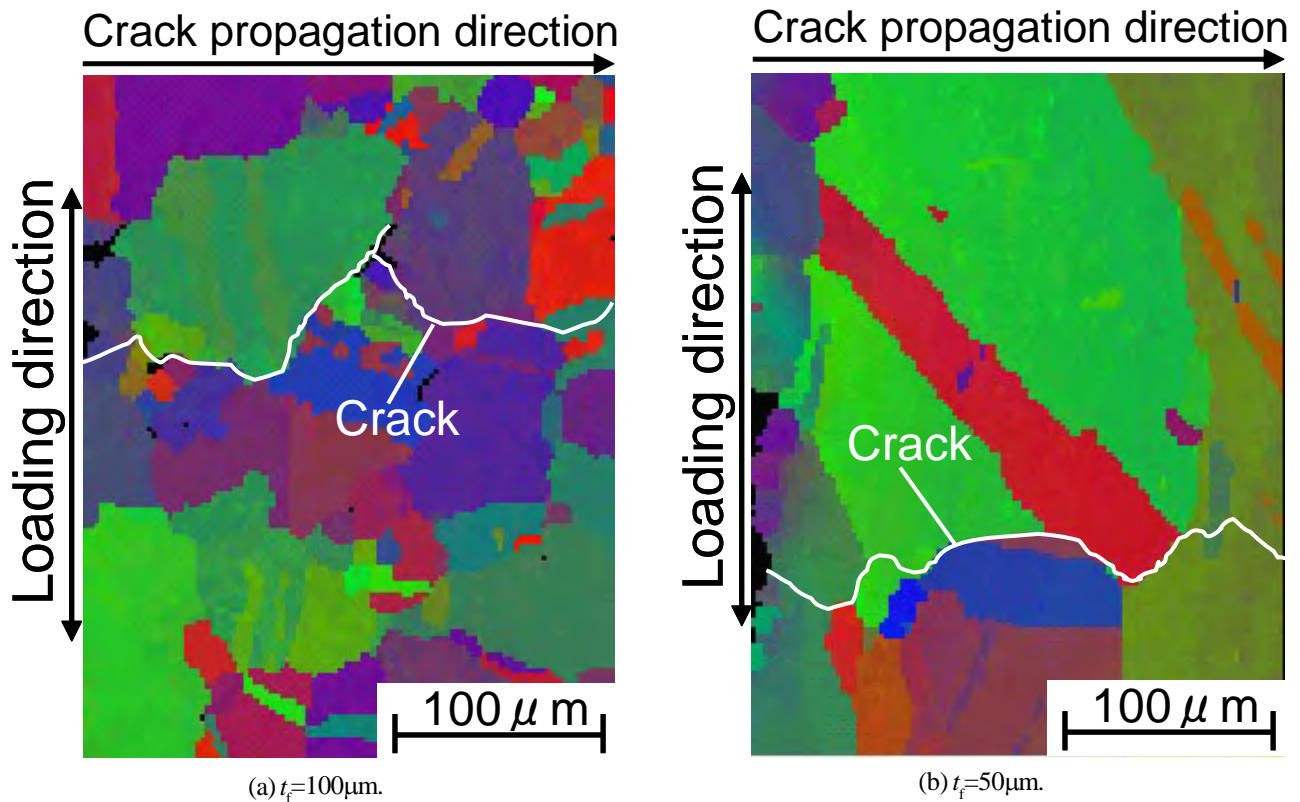

(a) t_f=100μm.

(b) t_f=50μm.

Fig. 8 Crystal orientation map obtained after fatigue testing.

short, the fatigue crack propagation was due to the slip deformation in the film of 50μm thickness, whereas the fatigue crack propagated with the crystal rotation in the film of 100μm thickness. As a result, it is considered that the fatigue crack propagates faster in the film with the thickness of 50μm than in that of 100μm thickness.

4. CONCLUSIONS

Copper films with the thickness of 100μm and 50μm were fatigued and the crystal rotation behavior with the fatigue testing was investigated by EBSD method. The main results obtained are as follows.
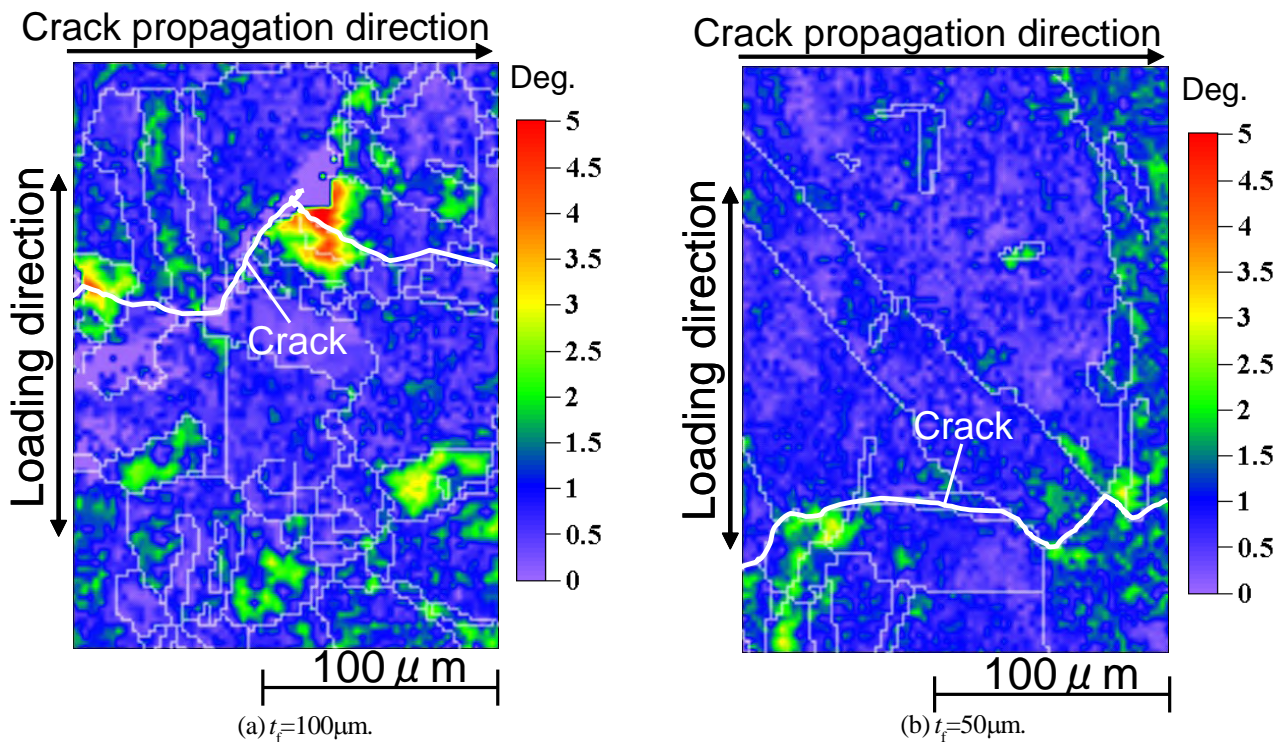(1) The crack propagates faster in the film of 50μm thick-

(a) t_f=100μm.

(b) t_f=50μm.

Fig. 9 Distribution of crystal rotation angle with fatigue testing.
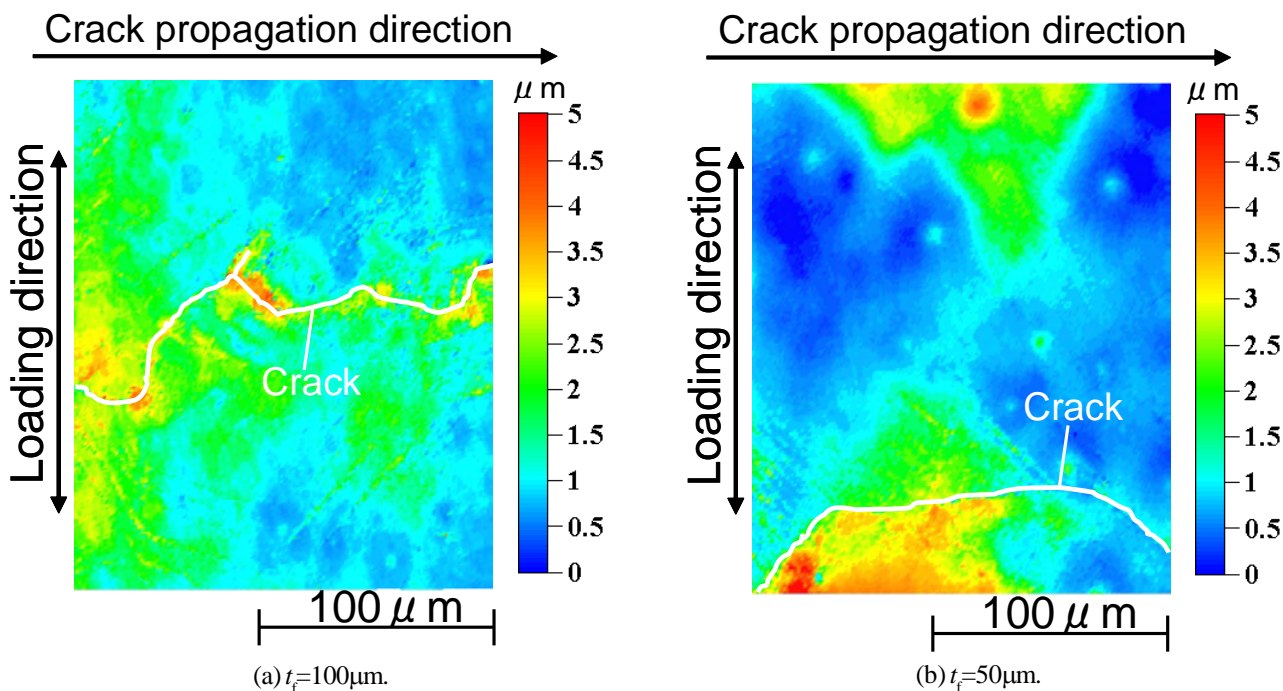

(a) t_f=100μm.

(b) t_f=50μm.

Fig. 10 Roughness around the fatigue crack measured by the confocal laser scanning microscopy.

ness than in that of 100μm thickness. While almost slip lines are localized near the fatigue crack in the film of 100μm thickness, large slip lines are scattered far from the fatigue crack in the film of 50μm thickness.

(2) The change of crystal orientation was remarkable near the fatigue crack in the film with the thickness of 100μm. On the other hand, the crystal rotation angle is relatively small even near the fatigue crack in the film of 50μm thickness.

(3) From the measurement by using the confocal lazer scanning microscopy, the film surface is piled up around the fatigue crack in the film with the thickness of 100μm. On the other hand, the difference in level is found across the fatigue crack in the film with the thickness of 50μm.

(4) The fatigue crack propagation was due to the slip deformation in the film of 50μm thickness, whereas the fatigue crack propagated with the crystal rotation in the film of 100μm thickness. As a result, it is considered that the fatigue crack propagates faster in the film with the thickness of 50μm than in that of 100μm thickness.

REFERENCES

[1] W. D. Nix, Metall. Trans. A, **20A**-11 (1989), 2217-2245.

[2] J. Oda, J. Sakamoto, T. Kubota and K. Yamada, Trans. Jpn. Soc. Mech. Eng., **57**-541A(1991), 2050-2056 (in Japanese).

[3] H. S. Hoffman, L. Griffiths, G. Monti and B. Singh, Advances in Electronic Packaging 1992, ASME, 1 (1992),23-26.

[4] T. Torii, K. Honda, A. Matsuba and M. Tanida, JSME Int. J., Ser. A, **39**-1 (1996), 34-41.

[5] T. Torii and K. Shimizu, Advances in Electronic Packaging 1999, ASME, 1 (1999), 867-874.

[6] T. Mura, Micromechanics of Defects in Solids, Martinus Nijhoff Publishers (1982), 63.

[7] V. Randle, Microtexture Determination and its Applications, The Institute of Materials (1992) , 11.

[8] K. Shimizu, T. Torii and T. Mori, J. Soc. Mater. Sci. Japan, **54**-9 (2005), 903-908.

[9] K. Shimizu, T. Torii and T. Mori, J. Soc. Mater. Sci. Japan, **54**-10 (2005), 1041-1046.